

SOME STUDIES OF LEAD FREE KNN-LN CERAMICS

A THESIS SUBMITTED IN PARTIAL FULFILMENT
OF THE REQUIREMENTS FOR THE DEGREE OF
MASTER OF SCIENCE IN PHYSICS

By

MALLIKA BHATTACHARYYA

Under the supervision of

Prof. Pawan Kumar



DEPARTMENT OF PHYSICS
NATIONAL INSTITUTE OF TECHNOLOGY
ROURKELA – 769008



NATIONAL INSTITUTE OF TECHNOLOGY ROURKELA

CERTIFICATE

This is to certify that the thesis entitled, “Some studies of lead free KNN-LN ceramic” being submitted by Mallika Bhattacharyya in partial fulfilments for the requirements for the award of Master of Science Degree in Physics Department at National Institute of Technology, Rourkela is an authentic work carried out by her under my supervision and guidance.

The work incorporated in this thesis has not been submitted elsewhere earlier, in part or in full, for the award of any other degree or diploma of this or any other institution or university.

Prof. Pawan Kumar
Dept. of Physics
National Institute of Technology

Date:
Rourkela-769008

ACKNOWLEDGEMENT

I would like to express my deep and sincere thanks to some people whose help make the present project work a success. At first I would like to thank my supervisor Prof. Pawan Kumar, Dept of Physics, N.I.T Rourkela. His constant encouragement, sincere help, support, patience, and inspiration help me to complete my Project work. I am extremely grateful for this intensive help and his continuous streams of ideas, which opened many avenues for study. I express my Gratitude, thanks and regard to him.

I am thankful to all the research scholars, especially Mr Prakash Palei at electro ceramics laboratory, for their friendship co-operation and encouragement.

Finally, I would like to thank my friends and my family who were constant sources of encouragement and inspiration during the whole period of carrying out the present project work.

Date:

(Mallika Bhattacharya)

CONTENTS

Topic	Page no
Abstract	5
Chap 1: Introduction	6
Chap 2: Literature survey & material selected	6 - 9
Chap 3: Optimization of synthesis process and Characterization techniques	10 - 16
3.1: steps of solid state route	10 - 12
3.2: Advantages of solid state route	12
3.3: experimental procedure	13
3.4: Characterization techniques	13 - 16
Chap 4: Results and discussions	17 - 23
4.1: XRD Analysis	17 - 18
4.2: SEM	18 - 19
4.3: Density Measurement	19
4.4: Dielectric Measurement	20 - 22
4.5: P-E loop	22 - 23
Chap 5: Conclusions	23
Chap 6: References	24 - 26

Abstract

Investigations in the development of lead-free $(1-x)(\text{K}_{0.5}\text{Na}_{0.5})\text{NbO}_3-x\text{LiNbO}_3$ piezoelectric ceramics have recently claimed comparable properties to the lead-based ferroelectric perovskites. The intrinsic nature of the dielectric and piezoelectric properties are discussed in relation to Curie temperature and morphotropic phase boundary (MPB) nature. To know the effect of LiNbO_3 substitution, lead-free $(1-x)(\text{K}_{0.5}\text{Na}_{0.5})\text{NbO}_3-x\text{LiNbO}_3$ (KNN:LN) ceramics were prepared by the solid-state reaction route. The crystallized phase and grain morphology of the KNN:LN ceramics were confirmed by X-ray diffraction and SEM studies, respectively. The dielectric and electrical properties were investigated as a function of the frequency and the temperature. Appearance of well saturated P-E loop confirms the ferroelectric nature of KNN-LN. The effect of LiNbO_3 substitution on crystallized phase, grain morphology, ferroelectric and electrical properties are discussed.

Chap 1: Introduction:

Ferroelectric materials were born in early 1940s with the discovery of the phenomenon of ferroelectricity as the source of unusually high dielectric constant in ceramic barium titanate capacitors. Since that time, these materials have been the heart and soul of several multibillion dollar industries, ranging from high-dielectric constant capacitors to later developments in piezoelectric transducers, positive temperature coefficient devices and electro-optic light valves. Materials based on two compositional systems, barium titanate and lead zirconate titanate have dominated the field through out the history. The more recent developments in the field of ferroelectric materials, such as medical ultrasonic composites, high-displacement piezoelectric actuators, photostrictors, and thin and thick films for piezoelectric and integrated-circuit applications have served to keep the industry young amidst its growing maturity [1, 2].

Chap 2: Literature Survey and Material selected:

Lead-based ferroelectric materials are the most commonly used piezoelectrics [3]. These materials include lead zirconate titanate $\text{PbZr}_x\text{Ti}_{1-x}\text{O}_3$ (PZT), $\text{PbMg}_{1/3}\text{Nb}_{2/3}\text{O}_3\text{-PbTiO}_3$ (PMN-PT), and $\text{PbZn}_{1/3}\text{Nb}_{2/3}\text{O}_3\text{-PbTiO}_3$ (PZN-PT) etc. Composition of these systems near their morphotropic phase boundaries (MPB) demonstrate high ferroelectric & piezoelectric properties [4,5]. In polycrystalline systems of these lead based systems piezoelectric charge coefficients (d_{33}) of up to 700 pC/N and single crystal of the lead-based materials of up to 1500-2500 pC/N have been reported [6,7&8]. Despite their excellent ferroelectric & piezoelectric properties these materials contain a large amount of lead (> 60 wt. %) which is toxic. Processing of these materials is normally accompanied by exposing or releasing the lead (Pb) into the environment. There are extensive environmental issues with restoring and recycling of the lead-based materials, since lead maintains for a long time in the environment and accumulates in living tissues, damages the brain and nervous system [9]. On the other hand, improper disposing of lead, such as disposing to open environment, could introduce it to the ecosystem and cause “acid rain”. Since the most successful piezoelectric ceramics are based on lead zirconates and lead

titanates, environmental concerns have been raised to find alternative ways to substitute with “lead-free” piezoceramics, particularly those with properties comparable with their lead-based counterparts. Furthermore, the necessity for using transducers with lead-free materials in therapeutic and monitoring ultrasound devices that requires the embedded system in the human body is another driving force for lead-free piezoelectric investigations.

Lead free ferroelectric materials are classified into four categories: (1) bismuth layered-structure, (2) tungsten bronze structure, (3) Pyrochlore structure and perovskite structure but special attention has been given to the perovskite structures. As it is easy to prepare and its structure is very simple than other structures. Lead-free ferroelectric materials with perovskite structure have general formula of ABO_3 . In this structure, cations based on their valence states and coordination numbers, occupy the A- or B- sites. Normally lower valency cations (1 to 3) occupy A- sites and higher valency (3 to 6) cations occupy B- sites. Bismuth sodium titanate $(Bi_{1/2}Na_{1/2})TiO_3$ and its solid solutions, $BaTiO_3$, and $KNaNbO_3$ -based ceramics (KNN-LN, KNN-LT) are some examples of perovskite structured lead-free ferroelectrics [10]. Lead zirconate titanate (PZT) is a lead based perovskite structured ferroelectric material. This is a binary solid solution of lead zirconate (PZ) an anti-ferroelectric (orthorhombic structure) and lead titanate (PT) a ferroelectric (tetragonal structure) material. This material possesses a morphotropic phase boundary (MPB) when the Zr/Ti ratio is $\sim 52/48$. Hence this material shows excellent piezoelectric and ferroelectric properties [4, 5]. Therefore, in the present study our focus is to search for a lead free material having a morphotropic phase boundary (MPB) with better ferroelectric and piezoelectric properties comparable to their lead based counter parts.

Sodium Potassium Niobate (NKN) is a solid solution of potassium niobate (KN) a ferroelectric and sodium niobate (NN) an anti-ferroelectric material. This material possesses a morphotropic phase boundary (MPB) when the Na/K ratio is $\sim 50/50$ [11]. Hence for this composition the piezoelectric, ferroelectric and electromechanical properties are maximized. $(Na_{0.5}K_{0.5})NbO_3$ shows piezoelectric properties of $d_{33}=80pC/N$, $K_p=36-40\%$, $Q_m=130$, and $\epsilon_r=290$ when it was prepared by ordinary sintering process. However, because of the hygroscopic nature of potassium oxide (K_2O) it is very difficult to synthesize unmodified Sodium Potassium Niobate (KNN) by conventional sintering [12]. Therefore, attempts have been made to improve the

sinterability and piezoelectric properties of KNN through the addition and/or substitution of several cationic elements in the A- or B-sites [13-20]. Kosec et al. showed that sinterability of the KNN could be improved by incorporation of excess amount of Nb^{5+} in B site or of Mg^{2+} in A site [21]. It is well known that densification rate is mainly influenced by the concentration of imperfections in crystal lattice [22]. It has also been reported that sinterability of ABO_3 lattice structure can be improved by A-site vacancy formation [3], which can be created either by having the excess B-ion or substituting the A-site with cation of higher valance. Malic et al. investigated the effect of the 0.5 mol. % A-site substituted alkaline earth dopants Mg^{2+} , Ca^{2+} , Sr^{2+} and Ba^{2+} on sinterability and electrical properties of the pure KNN [23]. In the case of Ca^{2+} and Sr^{2+} , he observed an improvement in densification and increase in permittivity and piezoelectric charge coefficient of about 11% and 17%, respectively over the un-doped KNN samples. The effect of ZnO on the microstructure and piezoelectric properties of KNN was studied by Park et al. [19]. Addition of ZnO showed a hardening effect by increasing the mechanical quality factor (Q_m) and coercive field (E_c). Introduction of ZnO improved the densification and resolved the deliquescency problem of pure KNN. The presence of liquid phase was reported in the microstructure, which could explain the higher densification and larger grain size of ZnO-doped KNN. Improvements in piezoelectric charge coefficient (d_{33}), planar coupling coefficient (k_p) and relative permittivity was achieved at 1 mol. % ZnO. Matsubara et al. studied the effect of new additives ($\text{K}_{5.4}\text{Cu}_{1.3}\text{Ta}_{10}\text{O}_{29}$; KCT, $\text{K}_4\text{CuNb}_8\text{O}_{23}$; KCN and KTaO_3 ; KT) on the sinterability and electromechanical properties of the KNN [15, 16, 17]. Addition of more than 0.38 mol. % KCT to KNN was effectively improved the densification of KNN ceramics. Presence of KCT provided the excess B-site ions along with formation of liquid phase during sintering to promote the densification. The effect of Ta^{5+} on the properties of the 0.38 mol.% KCT-doped KNN was also studied by Matsubara [17]. In spite of the “hard” piezoelectric characteristic of KCT, Ta^{5+} addition showed the softening behavior with large electrostrictive effect, which resulted in an improvement in k_p , relative permittivity, strain and d_{33} of doped KNN. Yamaguchi et al. investigated the Substitution of Li^{+1} in KNN for the composition of 0.38 mol.% of sintering aid KCT [18]. Incorporation of Li^{+1} in A-site increased the Curie temperature and lowered the orthorhombic-tetragonal phase transition temperature. Room temperature permittivity increased upon Li^{+1} substitution, however, maximum permittivity at

Curie temperature declined with higher concentration of Li^{+1} . Higher planar coupling coefficient, $k_p = 0.43$ and mechanical quality factor, Q_m : 2000 was obtained in 1 mol. % of Li^{+1} when it was substituted for K^{+1} site. Zhang et al. studied the effect of LiSbO_3 on KNN ceramics [24]. Combined effect of Li^{+} and Sb^{5+} decreased the orthorhombic-tetragonal phase transition temperature (T_{o-t}) but did not significantly reduce the Curie temperature (T_c). The key factor in enhancement of the polarizability and dielectric properties was the location of the orthorhombic-tetragonal phase transition (T_{t-o}) temperature. Addition of the Li^{+} and Sb^{5+} to KNN system shifted the transition temperature (T_{t-o}) to the room temperature where we observe high relative permittivity. Guo et al, studied the effect of Li^{+1} in the form of LiTaO_3 (simultaneously introducing the Li^{+1} and Ta^{5+}) also improved the electromechanical properties [25]. The morphotropic phase boundary (MPB) between orthorhombic and tetragonal phases was found at 5-6 mol. % of LiTaO_3 ; (LT). the piezoelectric constant d_{33} of 200 pC/N, planar coupling coefficient of 36% and relative permittivity of 580 were achieved at MPB composition ($x=0.05$). Kazuhiko et al. studied the effect of LiNbO_3 on KNN ceramics. He reported that the piezoelectric property is maximized at around the composition of 0.94KNN-0.06LN, that is around 200-235 pC/N and planar (K_p) and thickness (K_t) mode electromechanical coupling coefficients reaching 0.38-0.44 and 0.44-0.48, respectively [26].

From the above literature survey we concluded that among all the lead-free ferroelectric materials KNN-LN shows better piezoelectric, ferroelectric and electromechanical properties. Therefore, KNN-LN is the best lead-free ferroelectric material to replace the lead based ferroelectric materials.

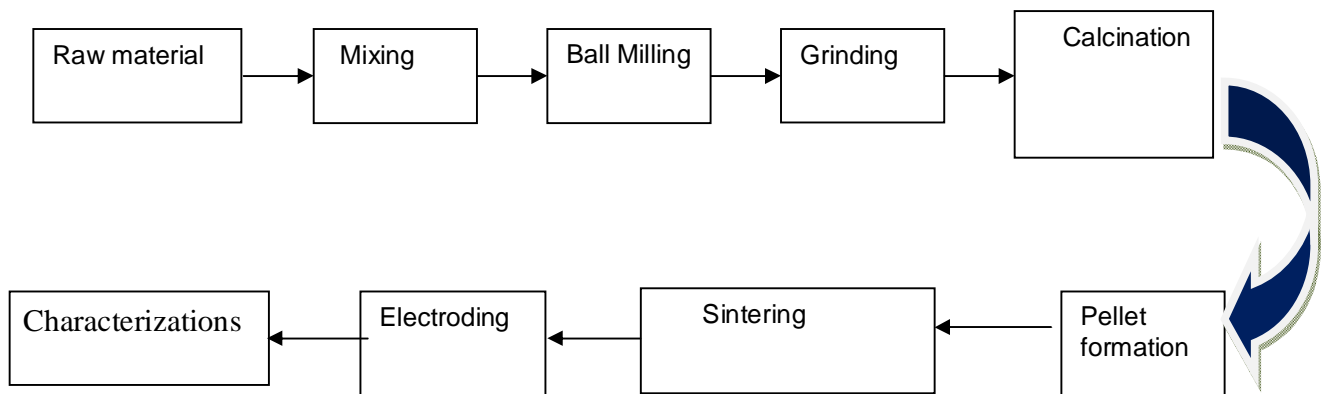
Research Objective:

The main goal of this work is to first synthesize $(1-x)\text{K}_{0.5}\text{Na}_{0.5}\text{NbO}_3-x\text{LiNbO}_3$ [$x=0.04, 0.05, 0.06$] ceramics in single perovskite phase. Optimization of sintering temperature in order to end up with a dense microstructure. Finally, an attempt has also been made to correlate structural and microstructural properties with the ferroelectric properties. The effect of LiNbO_3 concentration on the structural and electrical properties are also discussed.

Chapter 3: Optimization of synthesis process & characterization techniques:

3.1: Steps of solid state route:

Ferroelectric devices are typically fabricated from polycrystalline ceramics. This involves two steps; preparation of ceramic powders and sintering of the shaped structures. The flow chart for the oxide-mixing technique or solid state reaction technique is shown in Fig



Flowchart showing the solid state fabrication process of ceramics

Solid state synthesis process involves production of end products from an assemblage of finely divided solids i.e. powders by the action of heat. Each step of processing has to be carefully monitored and controlled to get the best product. The steps are as follows:

Raw materials:

The raw materials (metal oxides or metal carbonates) are first weighed according to the stoichiometric formula of the ferroelectric ceramics desired. The raw materials should be of high purity. The particle size of the powders must be in the submicron range for the solid phase reaction to occur by atomic diffusion.

Mixing:

Now the powders mixed either mechanically or chemically. Mechanical mixing is done by either ball milling or attrition milling for a short time. Chemical mixing is more homogeneous as it is done by precipitating the precursors in the same container.

Solid state synthesis process involves production of end products from an assemblage of finely divided solids i.e. powders by the action of heat. Each step of processing has to be carefully monitored and controlled to get the best product. The steps are as follows:

Calcination:

In this step the solid phase reaction takes place among the constituents by interdiffusion of their ions giving the ferroelectric phase. In this thermal process thermal decomposition, phase transition of solid materials takes place. It occurs above transition temperature for phase transition. At transition temperature the standard Gibbs free energy for a particular calcination reaction is equal to zero. The higher the calcining temperature the higher the homogeneity and density of the final ceramic product. Proper calcination temperature is necessary to obtain the best electrical and mechanical properties. In calcination process our aim is to remove [water](#) and CO_2 to form desired solid solution and as a consequence of reaction to have reduced volume shrinkage in the final firing.

Grinding:

The lumps produced from calcinations are grinded by mortar pestle.

Binder addition:

Binders, used in small concentrations, serve to provide bridges between the particles. In this way they aid the granulation of a powder (e.g. as the feed material for die compaction) and serve to provide strength in the green body.

Shaping:

The desired shape can be provided by various techniques including powder compaction, slip casting and extrusion. In powder compaction the powder is placed under high pressure to get

desired shape. Slip-casting is used to make large number of exact replicas of an original model. Extrusion is used to get the shape with fixed cross-sectional profile

Binder burnout:

Binder burnout is a processing step performed before sintering where the green body is heated at 600⁰C with soaking time for 2hr where the polymer binder is burnt out of the ceramic.

Sintering:

Sintering is the process by which ceramic bodies are fired at elevated temperature to achieve desired microstructure. Microstructure refers to density, grain shape, grain size and distribution, porosity, pore size and distribution. A full densification of ferroelectric ceramics ensures to achieve the maximized performance. The ‘driving force’ for densification is the reduction in surface energy as the free surfaces of particles disappear. Generally, the densities of ferroelectric ceramics increases with increasing sintering temperature. Sintering temperature is that temperature at which the grains of solid formed from powder start connecting through its boundaries and merges so forms a larger grain. It is generally between 2/3 rd. of melting temperature of that material.

Electroding:

Electroding involves application of a layer of metallic silver in dispersed liquid or paste form on the surface of the sintered pellets. Ideally the silver should adhere strongly to the ceramic, it should be very thin, practically zero resistance, and a good chemical and physical durability. The pellets are then heated to form a continuous conducting layer intimately bonded to the ceramic surface. Electrode adherence is critical. If there is any lack of intimate bonding, the gap between the electrode and the high dielectric constant ceramic acts as a series capacitance of low value.

3.2: Advantages of solid state route:

The final electromechanical properties of ferroelectric ceramics greatly depend upon the processing conditions of the ceramic. In the present study we will be employing the solid state reaction route for synthesizing the modified KNN-LN system. In this process; it is easy to synthesize the material and also it is economical. Each step of processing has to be carefully monitored and controlled to get the best product.

3.3: Experimental procedure:

Lead free (1-x)K_{0.5}Na_{0.5}NbO₃-LiNbO₃ (KNN-LN) [x=0.04-0.06] ceramics were prepared by a conventional solid state reaction route. Sodium carbonate (Na₂CO₃, 99% purity), potassium carbonate (K₂CO₃, 99% purity), lithium carbonate (Li₂CO₃, 99% purity), and niobium pentoxide (Nb₂O₅, 99% purity) were used as starting materials. Stoichiometric weights of all the powders were mixed and ball milled with acetone for 8 h, using zirconia balls as the grinding media. After drying the slurry in oven, the calcination was carried out at 850⁰C for 6 h and single phase formation was confirmed by the X-ray diffraction (XRD) technique. The calcined mixture was mixed thoroughly with 2wt% polyvinyl alcohol (PVA) binder solution and then pressed into disks of diameter ~10 mm and a thickness ~1.5 mm under ~60MPa pressure. The sintering of the samples was carried out at 1080⁰C, 1100⁰C and 1120⁰C for 4 h, respectively with a heating rate of 5⁰C/min in air. XRD analysis of the pellets were performed on a PW 3020 Philips diffractometer using Cu K α (λ =0.15405 nm) radiation in order to examine the phases present in the system. The sintered microstructures were observed using a JEOL T-330 scanning electron microscope (SEM). The bulk densities of the samples were measured by the Archimedes method. Silver paste was applied on both sides of the samples for the electrical measurements. Dielectric constant (ϵ_r) and dielectric loss ($\tan\delta$) were measured as a function of frequency and temperature using a computer interfaced HIOKI 3532-50 LCR-HITESTER. A conventional Sawyer–Tower circuit was used to measure the polarization hysteresis (P–E) loop at 20 Hz frequency.

3.4: characterization techniques:

Density measurement:

The experimental bulk density is measured by using Archimedes principle.

$$Density = \frac{D}{W - S} \times \rho_l$$

Where:

D- Dry weight,

W- Soaked weight and

S- Suspended weight.

ρ_l -Density of the liquid medium.

XRD (X-Ray Diffraction):

X-rays are electromagnetic wave in the spectrum between gamma-rays and the ultraviolet of wavelength about 1 Å. XRD is an important technique used to determine (a) Crystal Structure,(b) Crystallite Size and Micro strain, (c) Unit cell lattice parameters and Bravais lattice symmetry, (d) Texture/Orientation in polycrystalline or powdered solid samples, (e) Phase Composition of a Sample (Quantitative Phase Analysis: determine the relative amounts of phases in a mixture by referencing the relative peak intensities) etc. For phase identification, calcined powders and sintered green bodies are examined by X-ray diffraction.

SEM (Scanning Electron Microscope)

Scanning electron microscopy is used for inspecting topographies of specimens at high magnifications. It is a type of electron microscope that images the sample surface by scanning it with a high energy beam of electrons in reaster scan pattern. SEM inspection is often used in the analysis of die/package cracks and fracture surfaces, bond failures and physical defects on the die/ package cracks and fracture surface. SEM is a useful tool for observation of microstructure of ferroelectric ceramics.

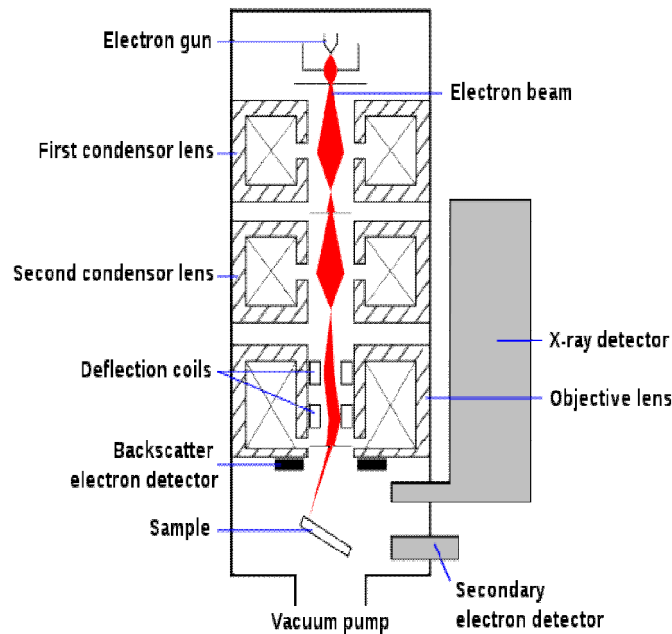


Fig 3(a) shows schematic diagram of SEM

Dielectric property study:

Ferroelectric ceramics generally have much higher dielectric constants, typically several hundred to several thousand. A LCR meter is a device that is used to measure the dielectric properties of ferroelectric ceramics.

P-E hysteresis loop:

The polarization versus electric field ($P \sim E$) has non linear relation for ferroelectric material and form a closed loop called as Hysteresis loop. Hysteresis loops can provide a plentiful amount of information for the understanding of ferroelectric materials. In paraelectric phase the P - E relation is linear and in ant ferroelectric phase it is double hysteresis loop. The domain concept is well explained by the phenomenon of hysteresis. A high remnant polarization is related to high internal polarizability, strain, electromechanical coupling etc. The coercive field indicates the grain size of a given material. A sudden large change in apparent polarization is usually indication of incipient dielectric Breakdown. [3]

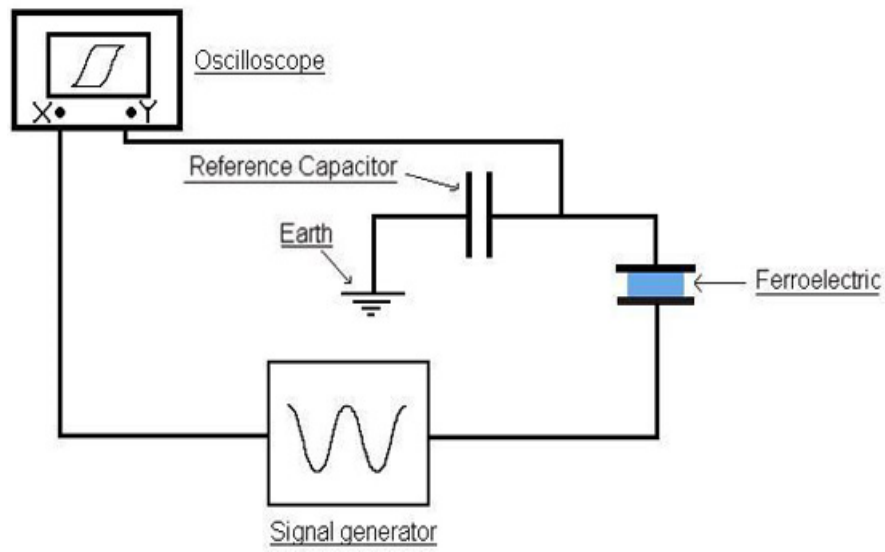


Fig 3(b) shows schematic diagram of Sawyer-Tower circuit

Chap 4: Result and discussion:

4.1: Structural analysis by XRD:

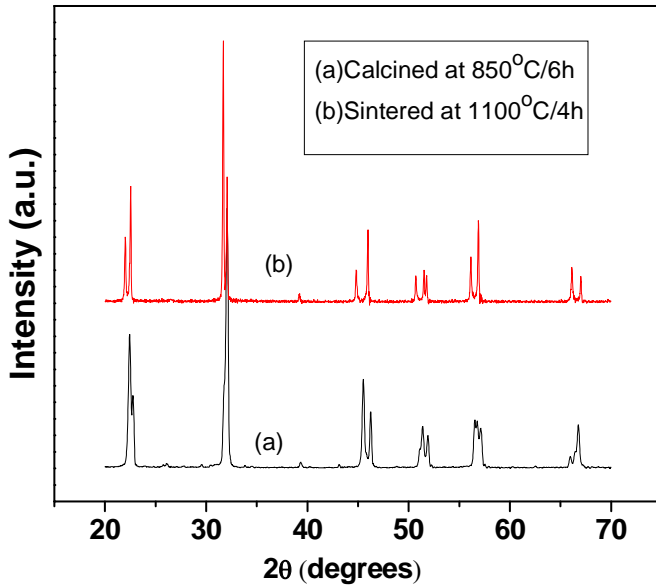


Fig.1(a)

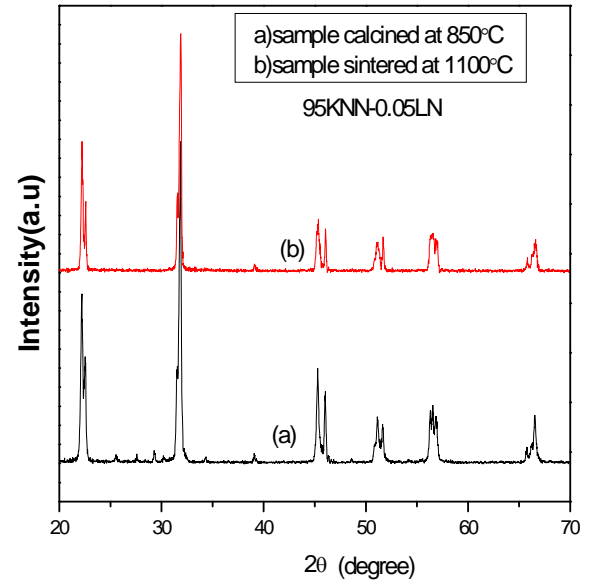


Fig.1(b)

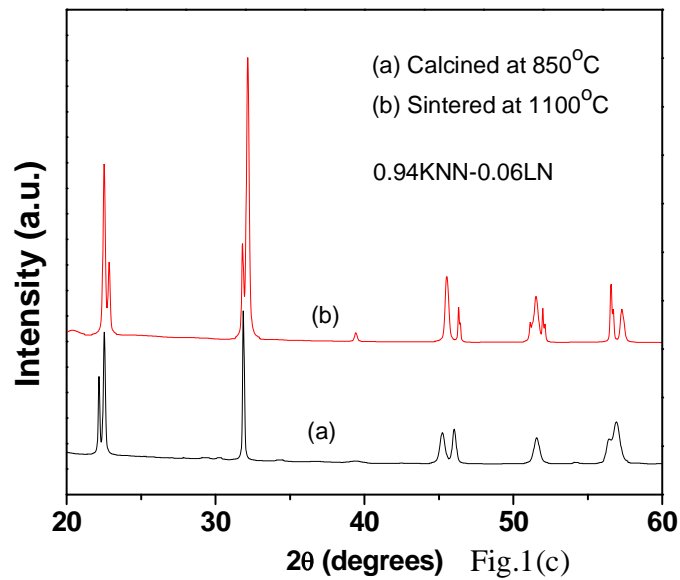


Fig.1(c)

Fig.1 XRD patterns of (a) 0.96KNN-0.06LN ceramics (b) 0.95KNN-0.05LN ceramics and (c) 0.94KNN-0.04LN ceramics.

Fig.1 shows the room-temperature X-ray diffraction (XRD) patterns of (a) 0.96KNN-0.04LN (b) 0.95KNN-0.05LN and (c) 0.94KNN-0.06LN samples calcined at 850°C and sintered at 1100°C.

The XRD peaks are found to be sharp and distinct indicating good homogeneity and crystallinity of the samples [26]. Single perovskite phase is developed in all the samples. The X-ray diffraction patterns of all the KNN-LN samples are indexed in different crystal systems and unit cell configurations using a computer program package 'Powdmult'. Standard deviations, S.D, $\sum \Delta d = (d_{\text{obs}} - d_{\text{cal}})$, where 'd' is inter-plane spacing, is found to be minimum for orthorhombic structure. The calculated lattice parameters and unit cell volume are listed in Table-1.

Sample	a (Å)	b (Å)	c (Å)	Vol. (Å ³)
0.96KNN-0.04LN	8.0286	7.8649	7.9947	504.83
0.95KNN-0.05LN	8.0053	7.8815	7.9807	503.52
0.94KNN-0.06LN	8.0017	7.8614	7.9166	497.99

It is noticed from Table-1 that with the increase in LiNbO₃ (LN) concentration the unit cell volume of the KNN-LN system decreases. This may be due to the fact that ionic radius of Li⁺(0.68 Å) is smaller than the ionic radii of (Na_{0.5}K_{0.5})⁺, hence decreases the volume.

4.2: Density measurement:-

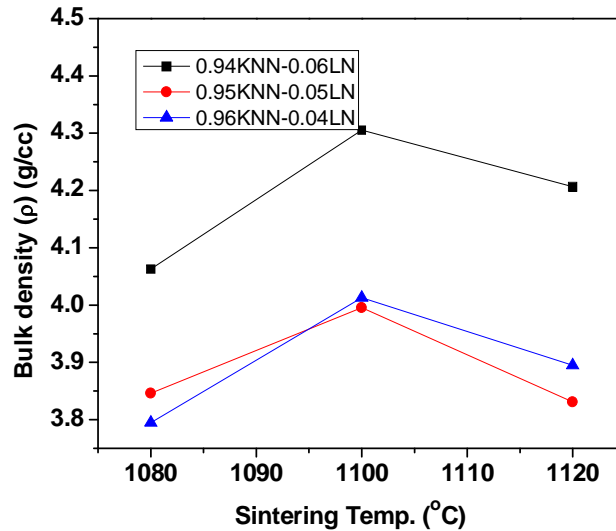


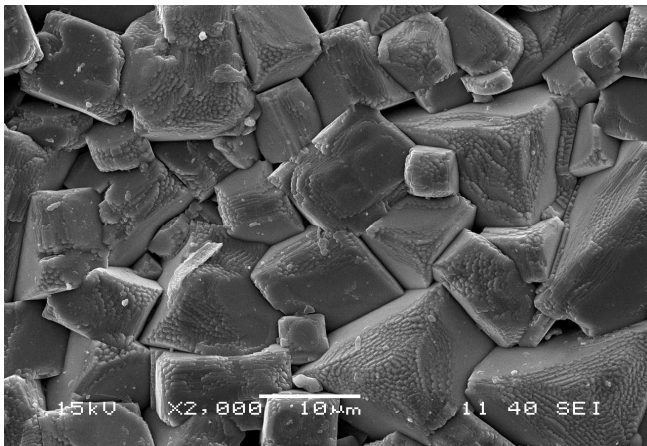
Fig.2 Bulk density of KNN-LN samples as a function of sintering temperature.

Fig.2 shows the bulk density (ρ) of all the KNN-LN samples as a function of sintering temperature. The bulk density of all the KNN-LN samples first increases with the increase in sintering temperature, and then decreases at 1120°C sintering temperature. Maximum density is obtained at 1100°C temperature in all the cases. The decrease in density of all the KNN-LN samples sintered at 1120°C may be due to the evaporation of potassium oxide at higher

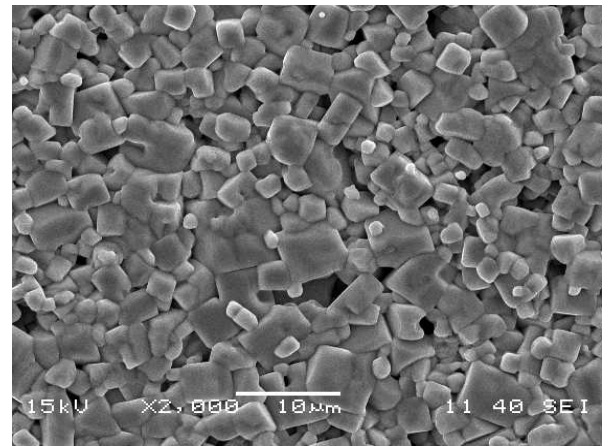
temperature, as it is volatile in nature [31]. Among all the KNN-LN samples, the 6% LN modified KNN ceramics possess higher bulk density $\sim 4.30\text{g/cc}$.

4.3: Microstructural study by SEM:

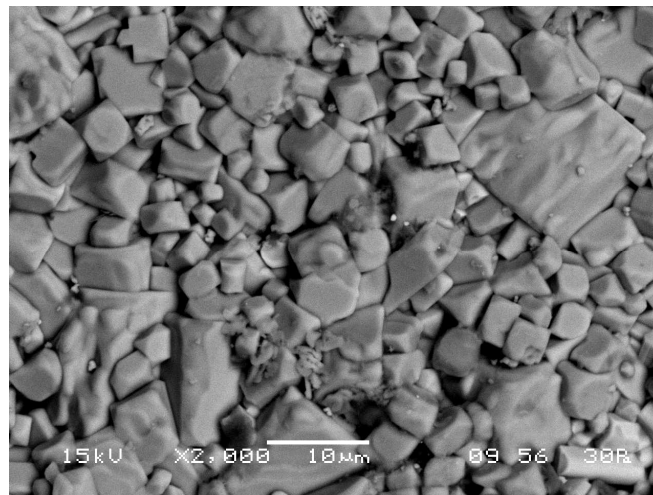
Fig.2 shows the SEM micrographs of (a) 0.96KNN-0.04LN (b) 0.95KNN-0.05LN and (c) 0.94KNN-0.06LN samples sintered 1100°C . Dense and non-homogeneous grains are observed in all the KNN-LN samples.



(a) 0.96KNN-0.04LN



(b) 0.95KNN-0.05LN



(c) 0.94KNN-0.06LN

Fig.2 SEM micrographs of (a) 0.96KNN-0.04LN (b) 0.95KNN-0.05LN and (c) 0.94KNN-0.06LN ceramics.

4.4: Dielectric measurements:

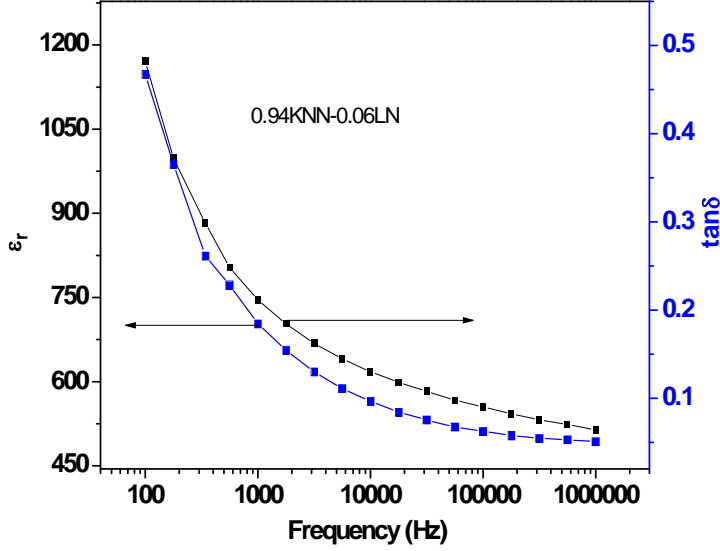


Fig.3(a)

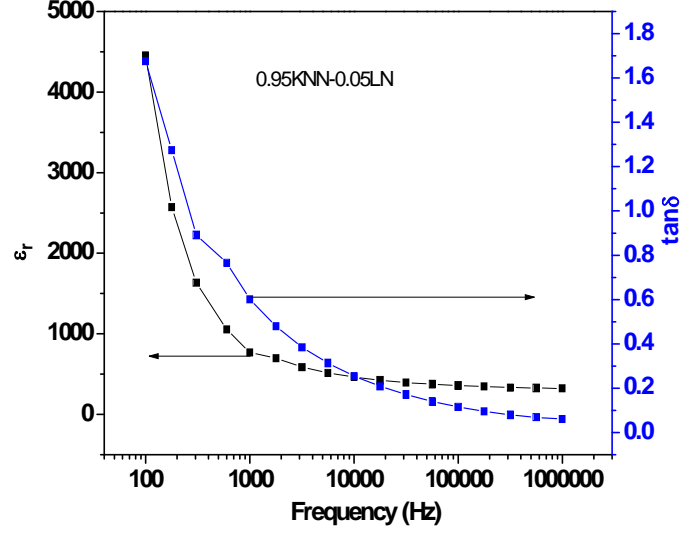


Fig.3(b)

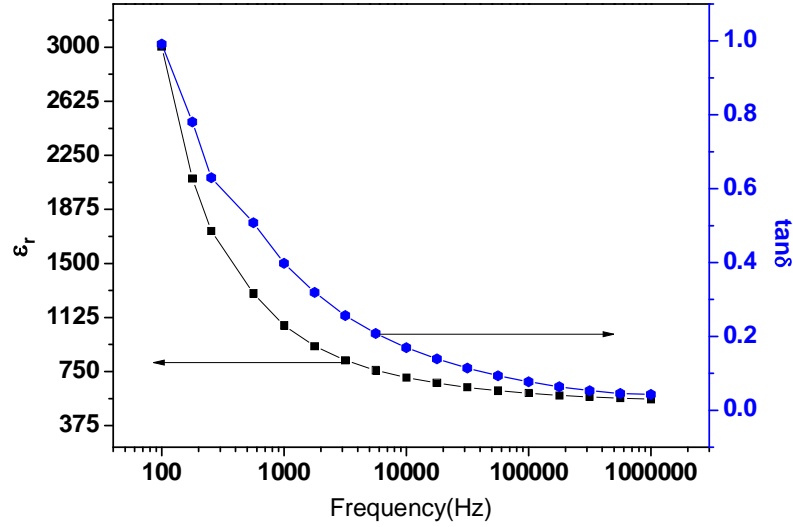


Fig.3(c)

Fig.3 Room temperature frequency dependence dielectric constant and dielectric loss of (a) 0.94KNN-0.06Ln (b) 0.95KNN-0.05LN and (c) 0.96KNN-0.04LN ceramics.

Fig.3 shows the frequency dependence of ϵ_r and $\tan\delta$ of all the compositions of KNN-LN samples. The room temperature value of ϵ_r at 1 MHz frequency of 0.94KNN-0.06LN, 0.95KNN-0.05LN and 0.96KNN-0.04LN samples are found to be ~520, 320 and 510 respectively whereas $\tan\delta$ values of are ~0.05, 0.065, and 0.045, respectively. It is observed that ϵ_r and $\tan\delta$ values of

all the KNN-LN samples decreases with the increase in frequency. The decrease in the value of ϵ_r can be explained on the basis of decrease in polarization with the increase in frequency. Polarization of a dielectric material is the sum of the contributions of dipolar, electronic, ionic and interfacial polarizations [33]. At low frequencies all the polarizations respond easily to the time varying electric field but as the frequency of the electric field increases different polarization contributions filters out, as a result, the net polarization of the material decreases which leads to the decrease in the value of ϵ_r . Further, the decrease of $\tan\delta$ with the increase in frequency can be explained by Debye formula [34]. According to this formula, at lower frequencies $\tan\delta$ is inversely proportional to frequency which explains the decrease in $\tan\delta$ with frequency [34]. The observed higher values of ϵ_r in case of 0.94KNN-0.06LN sample may be attributed to the higher bulk density in the sample.

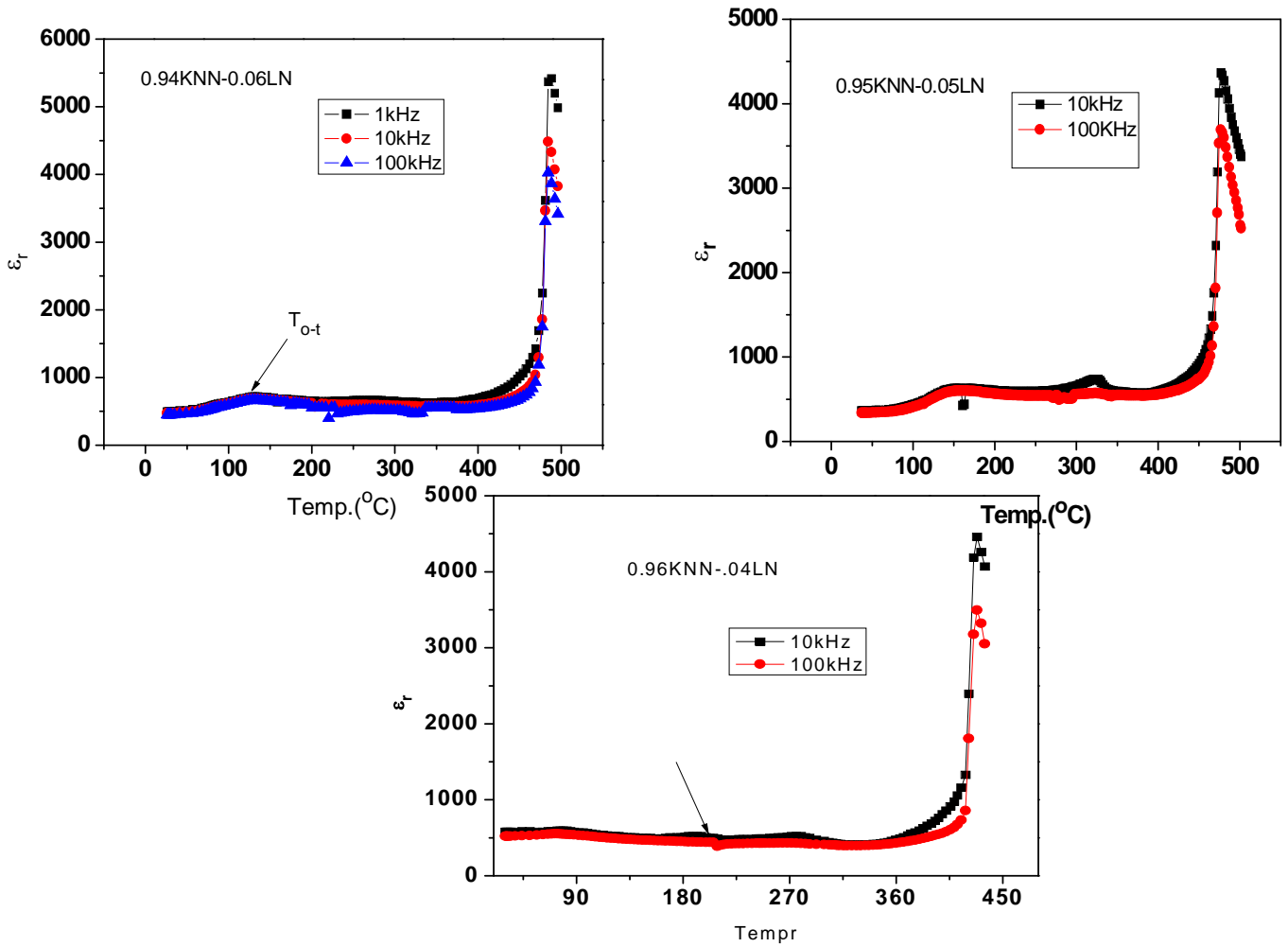


Fig.4 Temperature dependence of ϵ_r of all the KNN-LN samples.

The temperature dependence of ϵ_r of all the KNN-LN samples are shown in Fig.4. Unlike pure KNN ceramics, here in all the cases two phase transitions are observed. It is found that with the increase in LN concentration the curie temperature (T_c) of the KNN-LN ceramics increases which may be due to the high curie temperature of LN ceramics. The orthorhombic-tetragonal phase transitions of all the ceramics also decreases with increase in LN concentration. The T_c of all the KNN-LN ceramics are found to be $\sim 440^\circ\text{C}$, 470°C and 480°C for 0.96KNN-0.04LN, 0.95KNN-0.05LN and 0.094KNN-0.06LN ceramics respectively. It is seen that with increase in temperature in all the KNN-LN samples ϵ_r increases. In the high temperature region, higher value of ϵ_r may be due to the contributions from space charge polarization.

4.5:P-E loop:

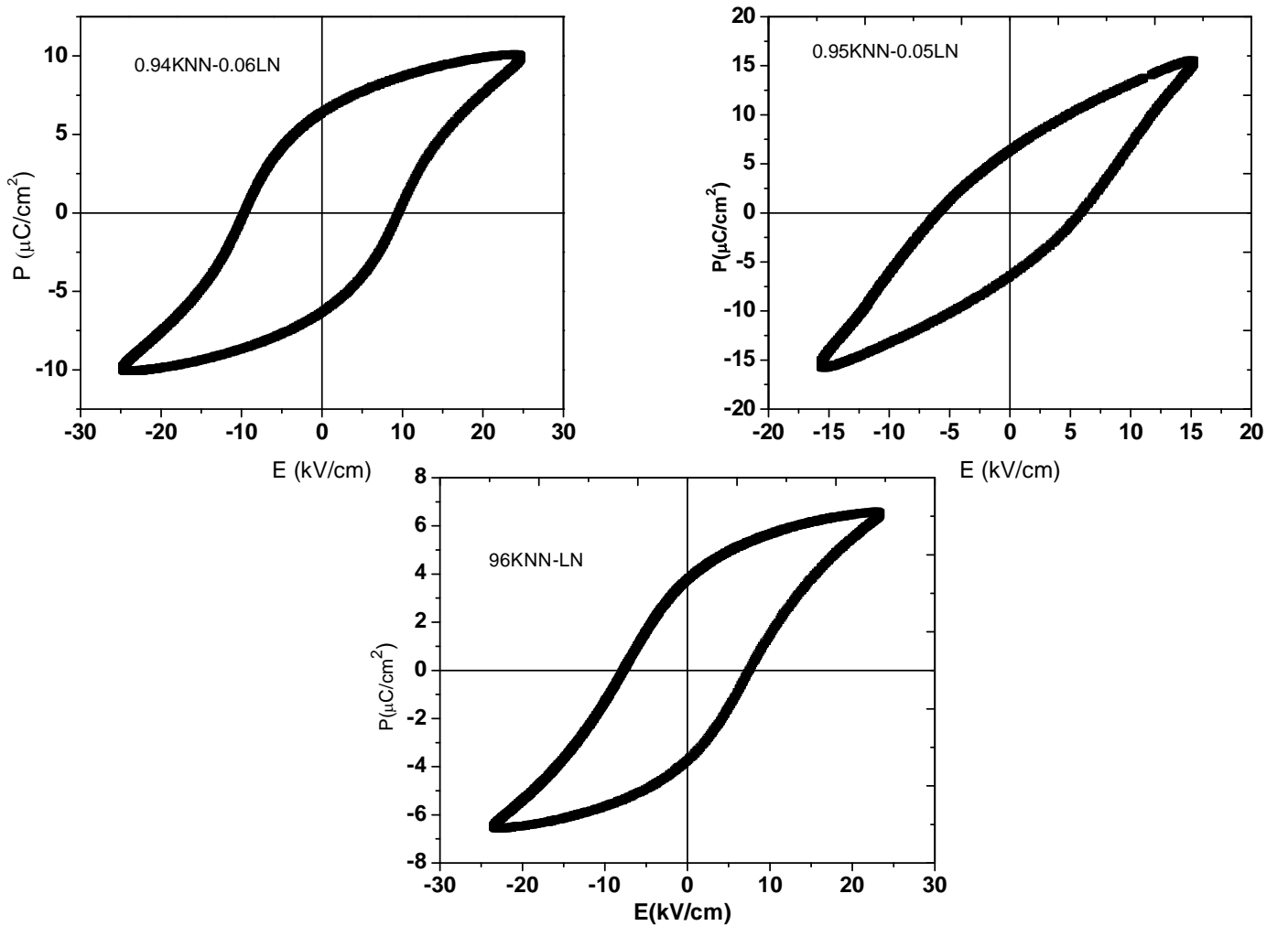


Fig.5 P-E loops of all the KNN-LN samples.

Fig. 5 shows the polarization vs electric field (P-E) hysteresis loops of all the KNN-LN ceramics. The development of hysteresis loops in all the KNN-LN samples confirmed the ferroelectric nature of the sample. Well saturated hysteresis loops are developed in case of the 0.94KNN-0.06LN and 0.96KNN-0.04LN samples. Highest value of remnant polarization is obtained in case of 0.94KNN-0.06LN sample which may be related to the higher density of the 0.94KNN-0.06LN ceramics.

Chap 5: Conclusions:

We have prepared $(1 - x)$ KNN – x LN where $x = 0.04, 0.05, 0.06$ by conventional solid state route. XRD analysis confirmed single perovskite phase and orthorhombic structure at room temperature. Unit cell volume decreased with increasing LN concentration. SEM micrographs show dense microstructures with low porosity in the samples with grain size in the 3-7 μ m range. Appearance of well saturated P-E loop confirmed the ferroelectric nature of KNN-LN ceramic. Curie temperature increased with increasing LN concentration. Higher dielectric constant at 1 MHz frequency is nearly about 520. 0.94 KNN – 0.06 LN has the maximum density of 4.30 amongst all the compositions. 0.94 KNN – 0.96 LN has the maximum remnant polarization of 6 μ C/cm².

Chap 6: References:

- [1] Gene H. Haertling “ferroelectric ceramics: History and Technology”
j.Am.Ceram.Soc.,82 [4],797- 818(1999)
- [2] G.Bush, “Early history of ferroelectricity”, 74,267-84 (1987).
- [3] B. Jaffe, W. R.Cook, and H. Jaffe, Piezoelectric Ceramics, Academic New York, Ch. 1,pp.1-5.,(1971)
- [4] H. Nagata, N. Chikoshi, T. Takenaka, “Ferroelectric Properties of Bismuth-Layered Structure Compound $\text{Sr}_x\text{Bi}_{4-x}\text{Ti}_{3-x}\text{Ta}_x\text{O}_{12}$ ”, Jpn. J. Appl. Phys., vol. 38, pp.5497-5499, (1999).
- [5] M. Suzuki, H. Nagata, J. Ohara, H. Funakubo and Takenaka, “ $\text{Bi}_{3-x}\text{M}_x\text{TiTaO}_9$ (M=La or Nd) Ceramics with High Mechanical Quality Factor Q_m ”, Jpn. J.Appl.Phys., vol. 42,pp. 6090-6093, (2003).
- [6] T. Sawada, A. Ando, Y. Sakabe, D. Damjanovic and N. Setter, “Properties of Elastic Anomaly in $\text{SrBi}_2\text{Nb}_2\text{O}_9$ -Based Ceramics” Jpn. J. Appl. Phys., vol. 42, pp. 6094-6098, (2003).
- [7] C. Duran, S. Trolier-McKinstry, and G. L. Messing, “Fabrication and electrical properties of textured $\text{Sr}_{0.53}\text{Ba}_{0.47}\text{Nb}_2\text{O}_6$ ceramics by templated grain growth”, J.Am. Ceram. Soc., 83, pp.2203-13, September (2000).
- [8] S. K. Haydon, D. A. Jefferson, “Quaternary Lead-Niobium-Tungsten Oxides Based on the Tetragonal Tungsten Bronze Structure”, J. Solid State Chem., 161, pp.135-151, (2001).
- [9] M. Demaeder, D. Damjanovic & N. Setter, “Lead-free piezoelectric materials”Journal of Electroceramics, 13, pp.385–392, (2004).
- [10] A.Safri, R.K. Panda and Victor F. Janas, “Ferroelectric ceramics: Processing, properties & applications”,Rutgers University, Piscataway NJ 08855, USA.
- [11] Thomas R. Shrout & Shujun J. Zhang, “Lead-free piezoelectric ceramics:

- Alternatives for PZT?,” J. Electroceramic, Vol. 19:pp.111–124, (2007)
- [12] Ruzhong Zuo and Jurgen Rodel, “sintering and electrical properties of lead free NKN piezoelectric ceramics”, J.Am.Soc., Vol. 89[6], 2010-2015 (2006)
- [13] S. Z. Ahn and W. A. Schulze, “Conventionally Sintered $(K_{0.5}Na_{0.5})NbO_3$ with Barium Additions”, Commun. Am. Ceram. Soc., vol. 70, C18-C21, (1987).
- [14] V. Bobnar, B. Malic, J. Holc, and M. Kosec, “Electrostrictive Effect in Lead-free-Relaxor $K_{0.5}Na_{0.5}NbO_3$ - $SrTiO_3$ Ceramic System”, J. Appl. Phys., vol. 98, (2005).
- [15] M. Matsubara, T. Yamaguchi, K. Kikuta, and S. Hirano, “Sinterability and Piezoelectric Properties of $(K,Na)NbO_3$ Ceramics with Novel Sintering Aid”, 43, No.10, pp.7159-7163, (2004).
- [16] M. Matsubara, T. Yamaguchi, K. Kikuta, and S. Hirano, “Sintering and Piezoelectric Properties of Potassium-Sodium Niobate Ceramics with Newly Developed Sintering Aid”, Jpn. J. Appl. Phys., 44, No.1A, pp.258-263, (2005).
- [17] M. Matsubara, K. Kikuta, and S. Hirano, “Piezoelectric Properties of $(K_{0.5}Na_{0.5})(Nb_{1-x}Ta_x)O_3$ - $K_{5.4}Cu_{1.3}Ta_{10}O_{29}$ Ceramics”, vol. 97, J. Appl. Phys., (2005).
- [18] M. Matsubara, T. Yamaguchi, K. Kikuta, and S. Hirano, “Effect of Li^{+1} Substitution on the Piezoelectric Properties of Potassium Sodium Niobate Ceramics”, Jpn. J. Appl. Phys., Vol. 44, No. 8, pp. 6136-6142, (2005).
- [19] S. H. Park, C. W. Ahn, S. Nahm, and J. S. Song, “Microstructure and Piezoelectric Properties of ZnO-added $(Na_{0.5}K_{0.5})NbO_3$ Ceramics”, Jpn. J. Appl. Phys., Vol. 43, No. 8B, pp. 1072-1074, (2004).
- [20] K. Kakimoto, I. Masuda, H. Ohsato, “Lead-free $KNbO_3$ Piezoceramics Synthesized by Pressure-less Sintering”, J. Euro. Ceram. Soc., 25, pp. 2719-2722, (2005).
- [21] M. Kosec and D. Kolar, “On Activated Sintering and Electrical Properties of $KNaNbO_3$ ”, Mater. Res. Bull., 10, pp. 335-340, (1975).
- [22] W. D. Kingery, H.K. Bown, D.R. Uhlmann, “Introduction to Ceramics”, John Willey and Sons, 2nd edition, (1976).
- [23] B. Malic, J. Bernard, J. Holc, D. Jenko, M. Kosec, “Alkaline-earth doping in

- (K,Na)NbO₃- based Piezoceramics”, J. Europ. Ceram. Soc., 25, pp. 2707-2711, (2005).
- [24] G. Zang, J. Wang, H. Chen, W. Su, C. Wang, P. Qi, B. Ming, L. Zheng, S. Zhang and T. Shrout, “Perovskite (Na_{0.5}K_{0.5})_{1-x}(LiSb)_xNb_{1-x}O₃ Lead-free Piezoceramics”, Appl. Phy. Lett.88, pp. 2129080-219083, (2006).
- [25] Y. Guo, Ken-ichi Kakimoto, H. Ohasto, “(K_{0.5}Na_{0.5})NbO₃-LiTaO₃ Lead-free Piezoelectric Ceramics”, Matt. Lett., 59, pp. 241-244, (2005).
- [26] Kazuhiko Higashide, Ken-ichi Kakimoto, H. Ohasto, “Temperature dependence on the Piezoelectric properties of (1-x)NKN-xLiNbO₃ ceramics”, J.Eu.,Soc.,13-15, Vol. 27,pp. 4107- 4110 (2007).
- [27] T. B. Weston, A.H. Webster, and V.M. Mcnamara, J.Am. Ceram. Soc., 52, 253 (1969)
- [28] N.Uchida, and T. Ikeda, Jap. J. Phys., 6, 1292 (1967)
- [29] F. Kulsar, J. Am. Ceram.Soc., 42, 343 (1959)
- [30] F. Kulsar, J. Am. Ceram.Soc., 48, 54 (1965)
- [31] R.B. Atkin, R.L. Holman, and R.M.Fularth, J. Am. Ceram.Soc.,54, 113 (1971)
- [32] H. Banno, and T. Tsunooka, Jap. J. Appl.phys., 6, 954, (1967)